Relaxation of Concentration Fluctuations in a Shear Field

Petr Štěpánek,*,† Wyn Brown,‡ and Søren Hvidt§

Institute of Macromolecular Chemistry, Academy of Sciences of the Czech Republic, Heyrovského nám. 2, 162 06 Praha 6, Czech Republic, Institute of Physical Chemistry, University of Uppsala, Box 532, S-751 21 Uppsala, Sweden, and Department of Chemistry, Roskilde University, DK-4000 Roskilde, Denmark

Received May 7, 1996; Revised Manuscript Received October 9, 1996[⊗]

ABSTRACT: We have investigated relaxations in a semidilute solution of a high molecular weight polystyrene in the vicinity of Θ conditions, using three different techniques: dynamic light scattering, relaxation of flow after cessation of shear recorded through the decay of the intensity of scattered light, and flow relaxation after cessation of shear recorded rheologically. We have used a solution at the Θ temperature of polystyrene with molecular weight $M_w = 4.9 \times 10^6$ in dioctyl phthalate. All three techniques yield similar values of the viscoelastic relaxation time, at various temperatures between 12 and 35 °C. Two additional modes are observed with dynamic light scattering: the well-established gel diffusion mode of the transient network of the entangled semidilute solution and an additional mode intermediate to the previous two. It is found that the shear field enhances only the longest viscoelastic relaxation mode.

Introduction

Entangled polymer solutions which are close to Θ conditions, i.e. close to phase separation, exhibit a substantial change in the intensity of the scattered light when subjected to shearing. Thus macroscopic shear flow strongly enhances concentration fluctuations and may even induce phase separation.[1,2] Dixon et al. have recently reported experiments on the dynamics of sheared polymer solutions[3,4] by making measurements of the transient response of the light scattering after cessation of shear for semidilute Θ state polymer solutions. Whereas they observed that dynamic light scattering (DLS) in equilibrium reveals two modes of relaxation for concentrations fluctuations, the shear flow was found to enhance only the slower q-independent, of these two modes. The DLS autocorrelation function of polymers of molecular weight of several million in poor solvents close to Θ conditions in semidilute solutions has been shown (see, for example, ref 5) to be multimodal, with a broad spectrum of relaxation times spanning over 8−9 decades. From this respect, the molecular weight used by Dixon is rather low, leading to correlation functions which consist of two narrow, easily separable contributions.

In principle, the concentration fluctuations will relax mainly through the cooperative motions of the transient network. Thus the high frequency limit of the spectrum is represented by a fast diffusive mode (i.e., its decay rate (Γ) is q^2-dependent, where q is the scattering vector) which is attributed to the relaxation of the collective motions of the network. The remainder of the concentration fluctuations decay through structural relaxation of the network. The slower modes, which have a very broad distribution, depend on the molecular weight of the polymer as well as on the concentration and are consequently independent of q. It is the present consensus that the slow, q-independent part of the spectrum is closely related to the viscoelastic properties of the transient network, although there is controversy as to their description.[6,7] The source of these effects apparently originates in the topological constraints which become effective above a certain minimum concentration and molecular weight necessary to produce entanglements.[8]

On a time scale shorter than the characteristic lifetime of the entanglements, the system will behave as a cross-linked network and there will be contributions to the longitudinal modulus both from the osmotic modulus and the elastic modulus of the network.[12,13] In the low-frequency limit, on the other hand, the chains can disentangle and the concentration fluctuations can relax like in a viscous solvent.

The gel diffusion coefficient D_g of the transient network can thus be written as

$$D_g = (1 - \phi)^2(K_{os} + M_{el})M/N_A cf \qquad (1)$$

where K_{os} is the osmotic bulk modulus, M_{el} the longitudinal elastic modulus of the transient network, ϕ polymer volume fraction, f the friction coefficient between a polymer molecule and the solvent, and N_A the Avogadro number. Inclusion of the $(1 - \phi)^2$ factor in eq 1 was discussed by Vink[9] and is also implicit in the derivation of the diffusion equation by Berne and Pecora.[10] We rederive briefly this equation in Appendix 1. In turn, M_{el} contains contributions from the bulk and shear elastic moduli,[11] K_{el} and G, respectively:

$$M_{el}(t) = K_{el}(t) + (4/3)G(t) \qquad (2)$$

In the simplest case, where the viscoelastic relaxation is characterized by a single exponential decay with relaxation time τ_v and amplitude M_o, we have

$$M_{el}(t) = M_o \exp(-t/\tau_v) \qquad (3)$$

The correlation function in such a case becomes double exponential[13,22]

$$g^1(t) = A_f \exp(-t/\tau_f) + A_s \exp(-t/\tau_s) \qquad (4)$$

The relative amplitude of the slow decay is given by[22]

$$A_s = M_o/(K_{os} + M_o) \qquad (5)$$

† Academy of Sciences of the Czech Republic.
‡ University of Uppsala.
§ Roskilde University.
⊗ Abstract published in *Advance ACS Abstracts,* December 1, 1996.

S0024-9297(96)00679-1 CCC: $12.00 © 1996 American Chemical Society

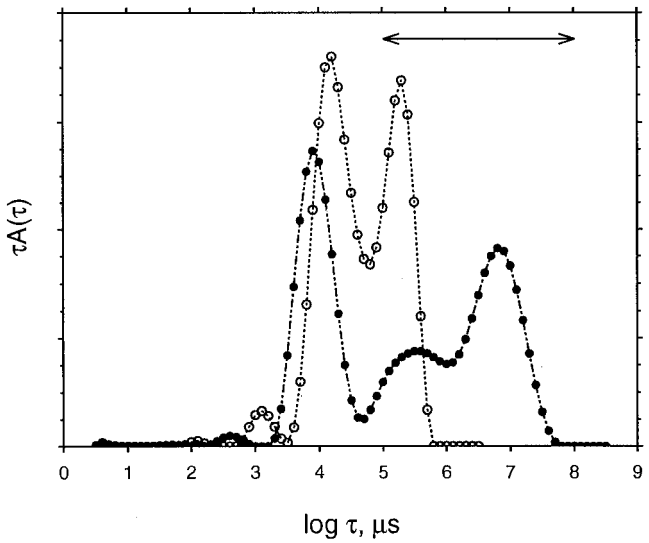

Figure 1. Distribution of decay times in $\tau A(\tau)$ obtained at a scattering angle of 90° for solutions of polystyrene in dioctylphthalate: (a) $M_w = 1.8 \times 10^6$, $c = 0.04$ g/mL (○) and (b) $M_w = 4.9 \times 10^6$, $c = 0.05$ g/mL (●). The arrows indicate the usable time window of the shear experiment; it is limited on the fast side to 0.1 s (which is the time needed to stop the shearing and the motion of the liquid[3]) and to ca. 100 s on the slow side, which is a reasonable duration of one accumulation.

Our earlier work[12] demonstrated that, whereas for a molecular weight of about $M = 10^6$ only two modes are represented in the relaxation time distribution, a broad spectrum of relaxational modes is present with higher molecular weights. In addition to that, for the polystyrene sample of molecular weight $M_w = 1.8 \times 10^6$, used in ref 3, $c^* = 0.03$ g/mL (using the empirically established expression[13] $c^* = 40/M^{0.5}$ for polystyrene), and therefore, the measurements on a sample with $c = 0.04$ g/mL were made at only $c/c^* = 1.34$; thus, the solution was not well-entangled, which is a prerequisite for measurements of this type. This issue is illustrated in Figure 1, which compares the spectrum of decay times obtained on a solution of polystyrene in DOP equivalent to that used in ref 3 ($M_w = 1.86 \times 10^6$, $c = 0.04$ g/mL) with that for a solution of higher molecular weight and concentration used in this work ($M_w = 4.90 \times 10^6$, $c = 0.05$ g/mL); for details, see the experimental section below. Clearly, the latter exhibits a more complex relaxation behavior than only two processes. The horizontal bar in Figure 1 delimits the usable time window of the cessation-of-shear experiment, as discussed below. It should be noted in particular that it is limited to 0.1 s on the fast relaxation side so that possible intermediate modes may not have been detected in the work described in ref 3. It is thus of some urgency to conduct further experiments along these lines to find out whether only the longest relaxational time is enhanced or whether the entire relaxational spectrum of viscoelastic modes is similarly modified.

Experimental Section

Materials. For shear measurements, polystyrene with molecular weight 4.9×10^6 (Toyo Soda Ltd.) was mixed directly with dioctyl phthalate (DOP, Merck) that was filtered through a 0.45 μm Millipore filter to make a single solution of polymer concentration $c = 0.05$ g/mL. The solution was allowed to reach equilibrium in an oven kept at 50 °C for a period of 2 months. The solution was then transferred to a transparent Couette cell placed in a Bohlin rheometer, as described below. A fraction of the solution was sealed in a dedusted cylindrical cell to be used for dynamic light scattering experiments. The reference sample used in Figure 1 was prepared using polystyrene with molecular weight 1.8×10^6 (Polyscience) dissolved in DOP at a concentration of 0.04 g/mL and filtered into a dedusted light scattering cell.

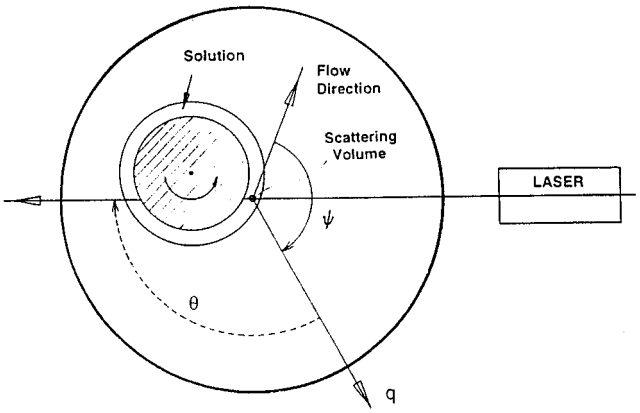

Figure 2. Scheme of the transparent Couette cell. θ is the scattering angle, whereas ψ is the angle between the flow direction and the recorded scattered beam.

Our recent experiments indicated that the value of the Θ temperature, Θ = 22 °C, quoted in the literature[14] may be too high. We have therefore used the standard static light scattering technique to determine the Θ temperature of the polymer/solvent system used in this work, as described elsewhere.[20] The fit to the experimental data in a standard Zimm diagram shows that the Θ temperature for the present system is Θ = 12 ± 0.5 °C. We have checked chromatographically and by NMR that the DOP we used contained no contaminants (which might decrease the Θ temperature) and we have analyzed the water content to be less than 0.07% (contamination by water would however increase the Θ temperature). The value of the Θ temperature is however unimportant for the purpose of the present study, since we are concerned only with relative changes of relaxation times.

Couette Cell. A specially constructed, transparent, all-glass rheometer cell in which the inner cylinder rotates was constructed (shown schematically in Figure 2). The latter was of high precision polished Pyrex made specially by Hellma (Mainz, Germany). The rotor was coupled to a driving unit (Bohlin VISCO 88 rheometer) via a 1:1000 gearing. The Couette cell was itself immersed in a bath of index-matching fluid (*trans*-decalin) with a thermostating coil to allow temperature control. Various temperatures between 15 and 35 °C were used. The Bohlin unit was computer-controlled and programmed to perform multiple operations. The cell assembly was mounted onto a static light scattering apparatus which has a He−Ne laser (35 mW) as the light source and which illuminated the gap between the rotor and the inner cylinder wall of the Couette cell. The scattered light was monitored by a photomultiplier coupled to the goniometer arm via a 100 μm fiber optic cable. A Hamamatsu photon counting device was used to process the signal.

An initial steady shear rate was applied (usually for the time $t_i = 20-60$ s) and then abruptly stopped and the scattered signal monitored for a time $t_i/5$ before and for 100s after cessation of shear. The cycle was repeated (typically 500−2000 times) in order to attain a good signal-to-noise ratio. The angle ψ between the flow direction and the scattered beam was not varied and was kept at $\psi = 45°$, since it was shown in ref 3 that the results of this kind of experiment do not depend on ψ. This was achieved by rotating the cell holder together with the photomultiplier arm. The scattering angle θ was varied between 45° and 120°.

Dynamical Rheology. Mechanical viscoelastic measurements were performed on a Bohlin VOR rheometer (Lund, Sweden) using a stainless steel Couette measuring cell C14 (inner diameter 14 mm, outer diameter 15.4 mm, and height 21 mm). The narrow gap ensures a virtually constant shear through the sample. The outer cylinder is surrounded by a water bath which is connected to a thermostat, and measure-

ments were performed at temperatures between 15 and 35 °C. The polymer solutions were allowed to flow into the measuring cell by gravity. The VOR instrument was used in the steady shear mode, where the outer cylinder rotates at a given rate. In flow relaxation experiments solutions were sheared at constant rate for a given period, and the relaxation of stress, $R(t)$, was then, after cessation of shear, monitored as a function of time.

Dynamic Light Scattering. A detailed description of the dynamic light scattering instrument was published earlier.[15] The polarized DLS measurements in the self-beating (homodyne) mode were made using a frequency-stabilized Coherent Innova Ar-ion laser operating at 488 nm with adjustable output power. The light was vertically polarized with a Glan-Thompson polarizer with extinction better than 10^{-6}. The detector optics employed a 4 μm diameter monomodal fiber coupled to an ITT FW130 photomultiplier, the output of which was digitized by an ALV-PM-PD amplifier/discriminator. The signal analyzer was an ALV-5000 digital multiple τ autocorrelator (ALV, Langen, Germany) with 288 approximately exponentially spaced channels. It has a minimum real-time sampling time of 0.2 μs and a maximum of about 100 s. The sample holder can be thermostated using an external circulation bath with available temperatures in the range −20 to 80 °C, with an accuracy of 0.1 °C.

Data Analysis. For dynamic light scattering, the measured intensity correlation function of scattered light, $g^2(t)$, is under standard conditions related to the field correlation function, $g^1(t)$, by the Siegert relation,

$$g^2(t) = 1 + \alpha|g^1(t)|^2 \tag{6}$$

where α is an instrumental factor. In turn, $g^1(t)$ is related by a Laplace transformation to the distribution of decay times, $A(\tau)$,

$$g^1(t) = \int A(\tau) \exp(-t/\tau)\, d\tau \tag{7}$$

To obtain $A(\tau)$ from the measured intensity correlation function $g^2(t)$, we have used the program[16,17] REPES which directly inverts $g^2(t)$. In all other aspects this program is similar to the widely used program[18] CONTIN which, however, operates on the field correlation function $g^1(t)$. All the diagrams of distribution functions in this work are plotted in the equal area representation, $\tau A(\tau)$ vs log τ. We have also used this program for the analysis of the flow relaxation data (both optical and mechanical), which are in the form[11]

$$F(t) = \int \tau A(\tau) \exp(-t/\tau)\, d\tau \tag{8}$$

The functional form of $F(t)$ is similar to that of $g^1(t)$, but the flow relaxation distributions are weighted by τ; the input routine of the program REPES has been modified to also accept $g^1(t)$ type data.

Results and Discussion

Shear Experiments. Figure 3a displays a typical time dependence of the scattered intensity, $I(t)$, from the polymer solution before and after cessation of shear, obtained at 15 °C at a scattering angle $\theta = 90°$ and a shear rate of $\dot{\gamma} = 0.26\ s^{-1}$. The value $t = 0$ corresponds to cessation of shear. Data with $t > 0$ have been analyzed by the REPES program as described above. Figure 3b shows the resulting distribution of relaxation times. There is only one component present in the distribution, indicating that only one process contributes to the relaxation with average relaxation time τ_R.

We may define the amplitude of this relaxation process as $B = (I(0) - I(\infty))/I(\infty)$, where for $I(\infty)$ we have taken the average of the last 100 points of $I(t)$. The amplitude decreases with decreasing shear rate. Figure 4 displays the dependence of B on the product $\dot{\gamma}\tau_R$. The amplitude becomes very small for $\dot{\gamma}\tau_R < 1$, which is

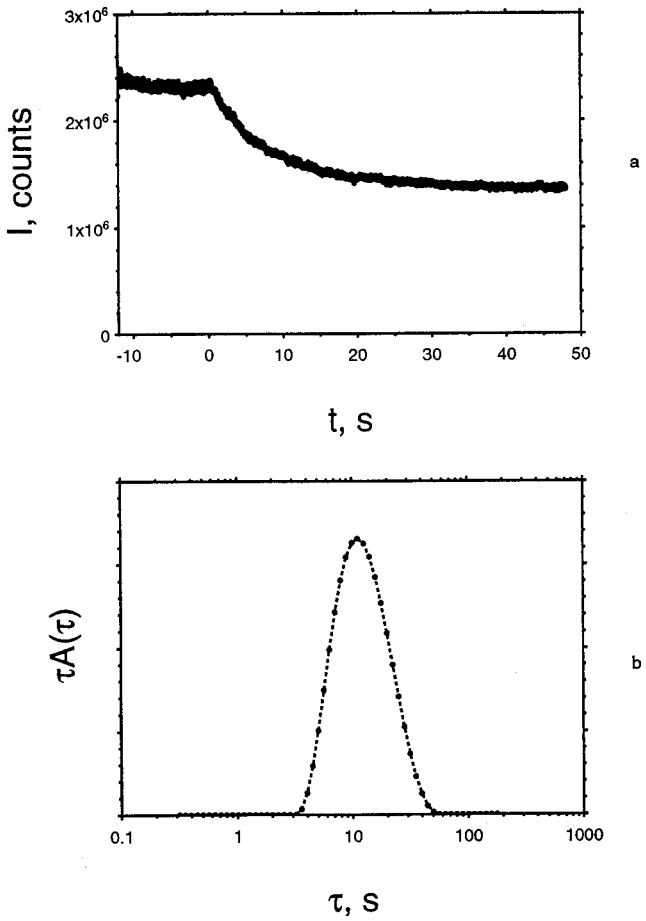

Figure 3. (a) Intensity of light scattered by the solution at 15 °C at a scattering angle of 90° as a function of time t before ($t < 0$) and after ($t > 0$) cessation of shear. (b) Distribution of relaxation times obtained from data shown in Figure 3a. The average relaxation time is $\tau_R = 13.8$ s.

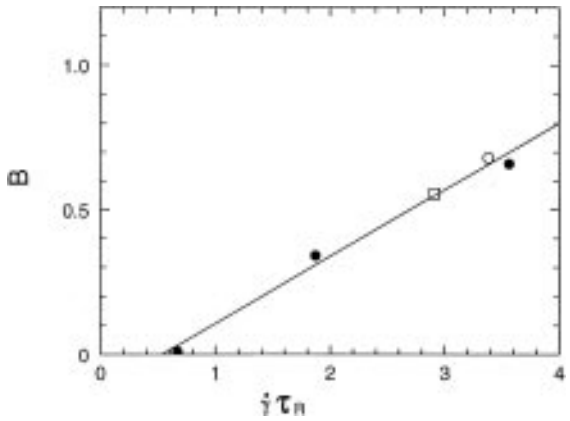

Figure 4. Dependence of the amplitude (B) of the optical stress relaxation signal on the $\dot{\gamma}\tau_R$, obtained at 15 °C (○), 35 °C (●), and 20 °C (□).

required[3] for a precise determination of τ_R, even for a large number of accumulations, on the order of 2000. In such a case, the signal-to-noise ratio is small and hinders reliable data analysis beyond a single exponential fit. Since our aim was to examine the possible existence of a more complex relaxation spectrum, we needed better quality data, even if τ_R is less well-determined, and therefore we have performed the majority of our experiments at values of $\dot{\gamma}\tau_R$ somewhat larger than 1. We have examined the flow relaxation curves as a function of shear rate and found that they always exhibit a single modal shape. Figure 5a shows

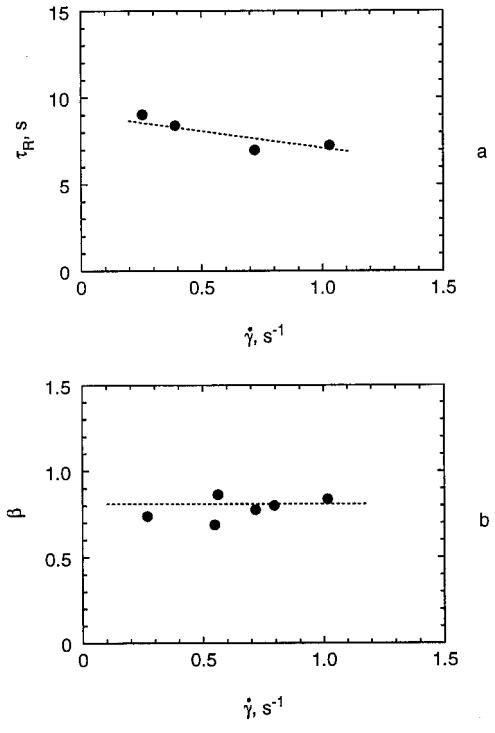

Figure 5. Dependence of (a) the average relaxation time, τ_R, and (b) the Williams−Watts parameter, β, on the shear rate $\dot{\gamma}$ for the investigated solution, at 20 °C and scattering angle 90°.

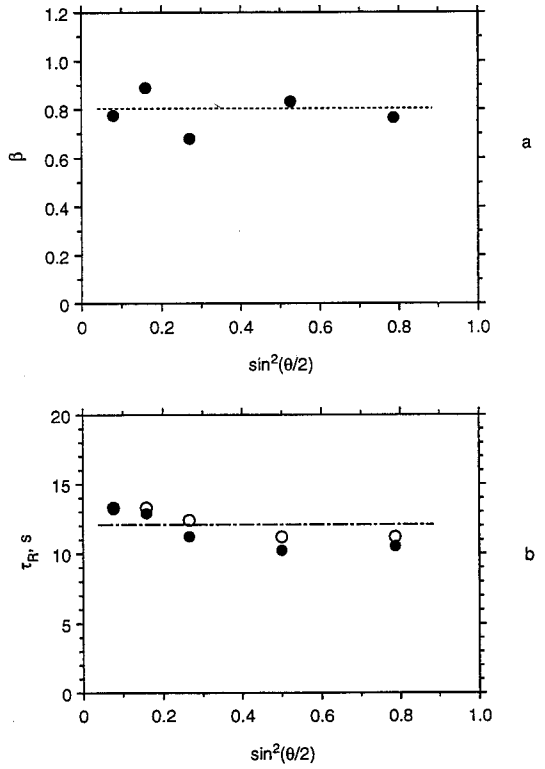

Figure 6. Dependence of (a) the Williams−Watts parameter, β, and (b) the average relaxation time, τ_R, on the scattering angle, θ, for the investigated solution, at the temperature of 20 °C.

the dependence of the corresponding relaxation time (τ_R) on the shear rate ($\dot{\gamma}$). The slight increase in τ_R with decreasing $\dot{\gamma}$ is unimportant for the present experiments, the main goal of which is to compare the complexity of the relaxation spectra obtained by relaxation of shear and by light scattering. This effect is more closely examined in a forthcoming publication[19] devoted to extraction of relaxation spectra from mechanical measurements. In order to check the width of the distribution of this component, we have fitted the flow relaxation curves, $F(t)$, with a Williams−Watts expression (the so-called stretched exponential),

$$F(t) = A_w \exp((-t/\tau)^{\beta}) + B_w \qquad (9)$$

where the parameter β describes the width of the distribution, and A_w and B_w are fitted parameters. Figure 5b shows that, within the scatter of the data, $\beta = 0.8$ for all shear rates. This is in reasonable agreement with data obtained rheologically (see Figure 8 below) and means that this relaxation process is somewhat broader than a single exponential. A more precise determination of β is not possible due to the relatively large noise in this type of experimental data.

The spectra of relaxation times have been determined for several angles at 20 °C. At all angles measured, only a single mode was observed with the β parameter in the vicinity of 0.8, as shown in Figure 6a, which supports the results of Figure 5b. The corresponding relaxation time, τ_R, is displayed as a function of scattering angle in Figure 6b. Within the experimental error, τ_R is independent of angle. This was expected since, as will be shown below, τ_R is equivalent to the longest viscoelastic relaxation time as determined by the mechanical flow relaxation experiment. The important observation is that only a single, relatively narrow relaxation process is detected.

The temperature dependence of the optical flow relaxation curves, $F(t)$, is shown in Figure 7a, for intensity recorded at a scattering angle 90°. As the temperature is decreased, τ_R increases, so the shear rate has to be decreased to keep $\dot{\gamma}\tau_R$ close to unity. This leads to an increased noise in the curves at low temperatures. The flow relaxation curves, $R(t)$, obtained rheologically in the same temperature range are displayed in Figure 7b. In both cases, a slowing down of the relaxation process with decreasing temperature is observed, which is due essentially to the increase in the viscosity of the solution. Figure 8a,b shows the temperature dependences of the relaxation time, τ_R, and of the β parameter obtained from these measurements. Both flow relaxation techniques exhibit a single mode relaxation spectrum in the vicinity of the Θ temperature,[20] $\Theta = 12$ °C, with the Williams−Watts parameter approximately equal to $\beta = 0.8$. The values obtained both for the average relaxation time, τ_R, and for the β parameter from both techniques are in good agreement. Further support for this finding is the fact that if we fit the dynamic light scattering data by a sum of a Gaussian function describing the gel mode and a stretched exponential to represent the slow and intermediate relaxations (see Figure 1 and details in the next section below), we obtain for the Williams−Watts exponent $\beta = 0.58$. On the β scale, this represents a substantial difference compared to the previous value. Moreover, such a fit yields a very poor distribution of residuals, indicating that a stretched exponential is not an appropriate description of the intermediate and is the slow part of the distribution of relaxation times observed in DLS. Figure 8b shows that the relaxation time τ_R increases as the temperature is decreased. This is also simply a consequence of the increased viscosity of the solvent; indeed, the reduced relaxation time, $\tau_R T/\eta$, is almost a constant independent of temperature, as demonstrated in Figure 8c. Thus no major viscoelastic

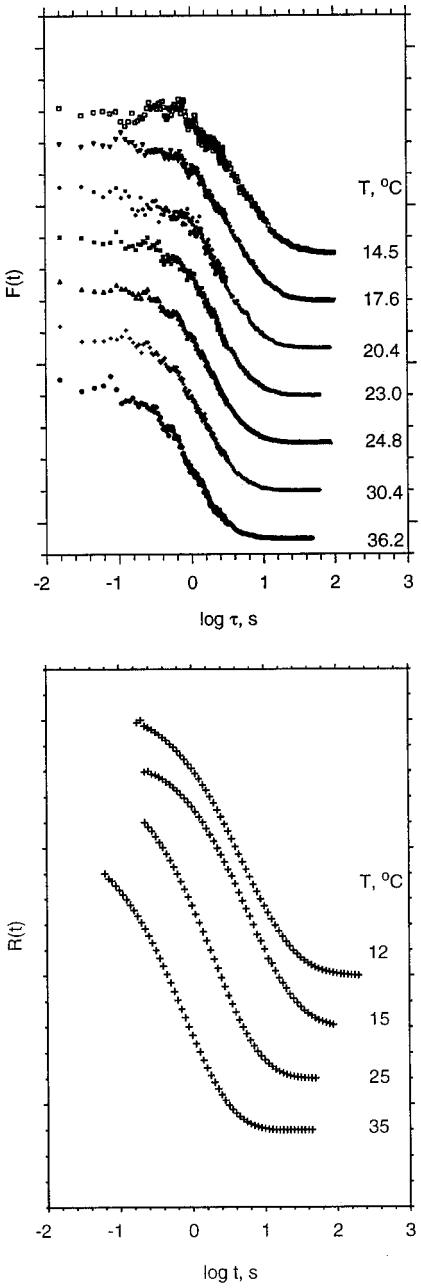

Figure 7. Temperature dependence of the flow relaxation curves measured (a) optically and (b) rheologically, for the solution investigated.

changes are observed when the solution approaches Θ conditions.

Dynamic Light Scattering. The spectra of relaxation times obtained on semidilute polymer solutions, such as those in Figure 1 above, have been published and discussed many times before; see, for example, ref 5, 6, 21, and 22. While these spectra are rather complicated for high molecular weight samples, two dominant features have been established:[5] (a) the dominant peak on the fast side of the distributions in Figure 1, with average relaxation time τ_g, corresponds to the gel diffusion mode of the entangled polymer network, and (b) the dominant peak limiting the slow side of the spectrum, with average relaxation time τ_R, represents the longest viscoelastic relaxation time.

Our purpose in this section is to compare the intermediate and slow parts of the distribution as obtained by the three techniques. We first consider the raw data, i.e. the relaxation curves obtained by the individual

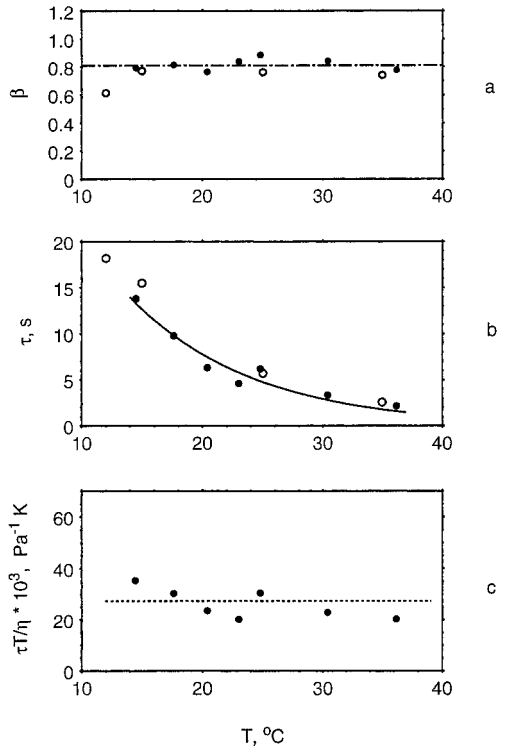

Figure 8. Temperature dependence of (a) the William−Watts exponent, β, (b) the average relaxation time, τ_R, from optical measurements (●) and rheological measurements (○), and (c) the reduced relaxation time, $\tau T/\eta$.

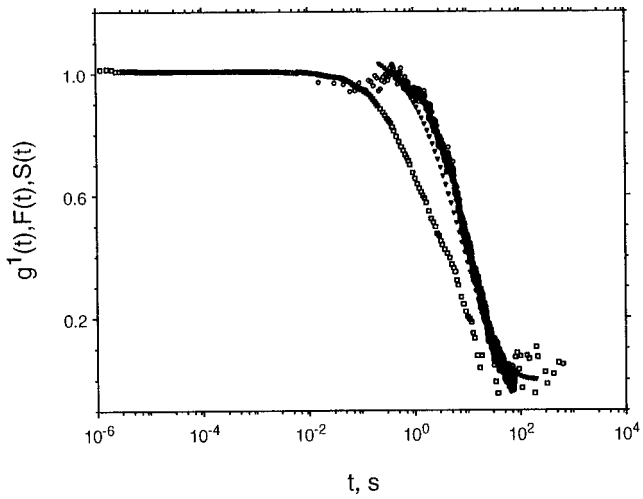

Figure 9. Relaxation functions obtained on the investigated solution by different experimental techniques, at 20 °C: optical relaxation (○), mechanical relaxation (▼), and dynamic light scattering (□).

techniques, $g^1(t)$, $F(t)$, and $R(t)$. The $g^1(t)$ function contains the gel diffusion component (the fastest peak in Figure 1), which is too fast to be accessible in the other two experiments. Thus, we have first subtracted the gel diffusion component from the $g^1(t)$ function according to the procedure explained in ref 23. Figure 9 displays the normalized relaxation functions obtained at 20 °C from the individual experiments. While there is good agreement between the mechanical and optical flow relaxation functions, the $g^1(t)$ function obviously contains additional faster decays.

The picture is more clearly visible in Figure 10 showing corresponding distributions of relaxation times. The peaks corresponding to the longest relaxation τ_R have been normalized to have the same height. There

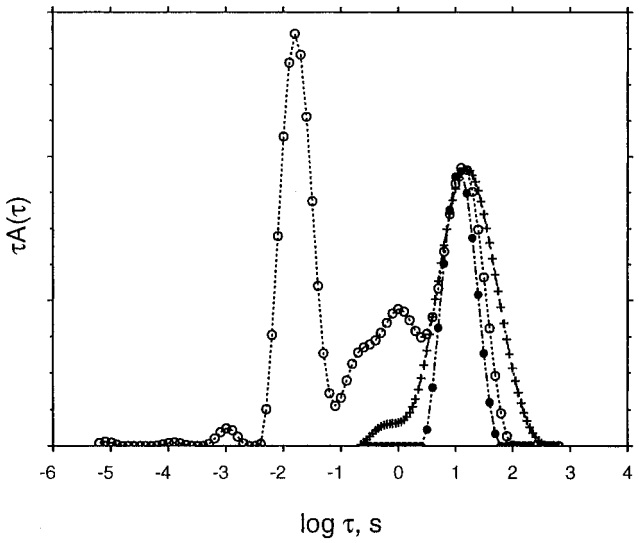

Figure 10. Distribution of relaxation times, $\tau A(\tau)$, obtained on the investigated solution at 20 °C from the relaxation functions shown in Figure 9: dynamic light scattering (○), optical relaxation (●), and mechanical relaxation (+).

are no significant components of the relaxation spectrum faster than τ_R. These results, which are an extension of the work presented in ref 3, demonstrate that, of the complex spectrum of relaxation times present in a semidilute polymer solution in a Θ solvent, it is only the longest viscoelastic relaxation time τ_R which is enhanced by a shear field. In dynamic light scattering, besides the cooperative diffusion coefficient, the possible existence of an intermediate mode has been documented earlier[24] on polystyrene/cyclohexane semidilute solutions, using a multiangle inverse Laplace transformation of correlation functions. Such analysis has shown the presence of an intermediate mode which is diffusive, i.e., its decay rate Γ is proportional to q^2 of which the origin has not yet been satisfactorily explained.

Conclusions

We have determined the longest viscoelastic relaxation time of a well-entangled semidilute polymer solution by observing the relaxations after cessation of shear and compared them to results of dynamic light scattering measurements. The values of the longest viscoelastic relaxation time as obtained by the different techniques are in good agreement. No faster relaxations were observed by both shear methods. The slight dependence of τ_R on $\dot{\gamma}$ determined by the shear experiments has no influence on the results of this comparison. Thus we also extend and corroborate the results of Dixon et al.,[3] who have shown that shear selectively enhances only the longest viscoelastic relaxation mode.

Acknowledgment. The authors gratefully acknowledge support of the Grant Agency of the Academy of Sciences of the Czech Republic through grant No. 450416, and support of the Swedish Natural Science Research Council (NFR).

Appendix 1

Equation 13.5.19 on page 337 of ref 10 reads

$$D = \frac{(1-\phi_s)c_s}{N_A f_s}\left(\frac{\partial \mu_s}{\partial c_s}\right)_{T,P} \tag{10}$$

with $\phi_\omega = (1-\phi_s)$. Here ϕ is the volume fraction, μ the chemical potential, f the friction coefficient, the subscript ω refers to the solvent and the subscript s refers to the polymer (solute). N_A is the Avogadro number. Next, we convert $(\partial\mu_s/\partial c_s)_{T,P}$ into the derivative of osmotic pressure. Since $\pi = -\mu_\omega/v_\omega$, we have

$$\left(\frac{\partial \pi}{\partial c_s}\right) = \left(\frac{\partial \mu_\omega}{\partial c_s}\right)\left(\frac{1}{v_\omega}\right) \tag{11}$$

Using the Gibbs−Duhem relation, $c_s\, d\mu_s = -c_\omega\, d\mu_\omega$, we obtain

$$\left(\frac{\partial \pi}{\partial c_s}\right) = +\left(\frac{\partial \mu_s}{\partial c_s}\right)\left[\frac{c_s}{c_\omega v_\omega}\right] \tag{12}$$

from which we get

$$\left(\frac{\partial \mu_s}{\partial c_s}\right) = \left[\frac{(1-\phi_s)}{c_s}\right]\left(\frac{\partial \pi}{\partial c_s}\right)_{T,P} \tag{13}$$

and finally we insert this into eq 10

$$D = \left[\frac{(1-\phi_s)^2}{N_A f_s}\right]\left(\frac{\partial \pi}{\partial c_s}\right)_{T,P} \tag{14}$$

References and Notes

(1) Hashimoto, T.; Kume, T. *J. Phys. Soc. Jpn.* **1992**, *61*, 1839.
(2) Onuki, A. *J. Phys. Soc. Jpn.* **1990**, *59*, 3427.
(3) Dixon, P. K.; Pine, D. J.; Wu, X.-L. *Phys. Rev. Lett.* **1992**, *68*, 2239.
(4) Wu, X.-L.; Pine, D. J.; Dixon, P. K. *Phys. Rev. Lett.* **1991**, *66*, 2408.
(5) Brown, W.; Nicolai, T. In *Dynamic Light Scattering: The Method and Some Applications*; Clarendon Press: Oxford, 1993; Chapter 6.
(6) Brown, W.; Stepanek, P. *Macromolecules* **1993**, *26*, 6884.
(7) Wang, C. H. *J. Chem. Phys.* **1995**, *102*, 6537.
(8) Jian, T.; Vlassopoulos, D.; Fytas, G.; Pakula, T.; Brown, W. *Colloid Polym. Sci.*, submitted.
(9) Vink, H. *J. Chem. Soc. Faraday Trans.* **1985**, *81*, 1725.
(10) Berne, B., Pecora, R. *Dynamic Light Scattering*; J. Wiley: New York, 1976.
(11) Ferry, J. D. *Viscoelastic Properties of Polymers*; J. Wiley: New York, 1970.
(12) Nicolai, T.; Brown, W.; Johnsen, R. M.; Stepanek, P. *Macromolecules* **1990**, *23*, 1165.
(13) Adam, M.; Delsanti, M. *Macromolecules* **1985**, *18*, 1760.
(14) Berry, G. G. *J. Chem. Phys.* **1967**, *46*, 1338.
(15) Schillen, K.; Brown, W.; Johnsen, R. M. *Macromolecules* **1994**, *27*, 4825.
(16) Jakes, J. *Czech. J. Phys.* **1988**, *38*, 1305.
(17) Jakes, J. *Collect. Czech. Chem. Commun.* **1995**, *60*, 1941.
(18) Provencher, S. W. *Makromol. Chem.* **1979**, *180*, 201.
(19) Hvidt, S., Brown, W. *Macromolecules*, in preparation.
(20) Nicolai, T.; Brown, W. *Macromolecules* **1996**, *29*, 1698.
(21) Brown, W.; Stepanek, P. *Macromolecules* **1992**, *25*, 4359.
(22) Nicolai, T.; Brown, W. In *Light Scattering: Principles and Developments*; Clarendon Press: Oxford, 1996; Chapter 5.
(23) Stepanek, P.; Johnsen, R. M. *Collect. Czech. Chem. Commun.* **1995**, *60*, 1941.
(24) Provencher, S. W.; Stepanek, P. *Part. Part. Syst. Charact.* **1996**, *13*, 291.

MA960679K